ELSEVIER

Marine Geology 129 (1995) 25–46

MARINE GEOLOGY
INTERNATIONAL JOURNAL OF MARINE GEOLOGY, GEOCHEMISTRY AND GEOPHYSICS

Morphodynamic evolution of a macrotidal barrier estuary

Guilherme Lessa [1], Gerhard Masselink [2]

Coastal Studies Unit, The University of Sydney, Australia

Received 2 May 1994; revision accepted 26 June 195

Abstract

The morphodynamics and recent geological evolution of a small barrier estuary were investigated. The estuary is located on the macrotidal central Queensland coastline and is characterised by an almost infilled back-barrier basin colonised by mangroves. The tidal channels inside the estuary account for less than 20% of the total estuarine area.

The vertical tide in the estuary is characterised by a positive asymmetry, where a rapid rise in water level during the flooding tide is followed by a slow fall in water level during the ebbing tide. The positive tidal asymmetry is predominantly ascribed to the truncation of the low tide level within the estuary due to the presence of a natural sill at the mouth of the estuary. The tidal asymmetry increases with increasing tide range and would suggest that the morphodynamics of the estuary are governed by flood tidal currents and flood-dominant sediment transport. However, flood-dominance is only observed during neap and mean tides. During spring tides, a large volume of water inundates the mangrove area at high tide and the consequent drainage of the mangrove area during the falling tide induces significantly stronger ebb flows and ebb-dominant sediment transport. Although the proportion of tidal cycles during which net ebb-directed sediment transport prevails is limited, on an annual basis the estuary can be considered ebb-dominant.

The stratigraphy of the estuary is characterised by a seaward-thickening wedge of open-marine sand up to 3 m thick, embedded between two layers of muddy sediments. The open-marine sand accounts for a significant part of the infilled volume and suggests that flood-dominant sediment transport has occurred during the infilling process. Hydrodynamic measurements indicate ebb-dominance for much of the estuary, suggesting that a hydrodynamical change from flood- to ebb-dominance has occurred during estuarine evolution. This hydrodynamical change may have resulted from an increase in intertidal water-storage capacity, predominantly through lateral mangrove-expansion, causing faster flow velocities during the ebbing tide. Ebb-dominance was probably first established at the head of the estuary and migrated downstream as the estuary became infilled.

1. Introduction

Barrier coasts often abut topographical depressions that are connected to the ocean through tidal inlets. Depending on their age, sediment availability, sea-level history and geological characteristics of the antecedent topography, these depressions may range from open-water lagoons to sediment-infilled salt-marshes. It is generally accepted that under conditions of minimal sea-level rise, salt-marshes (mangrove counterparts in temperate zones)are the final stage of an evolutionary cycle that starts with an open-water lagoon (Lucke, 1934; Newman and Munsart, 1968; Roy, 1984;

[1]Present address: Centro de Estudos do Mar, UFPR, Pontal do Sul, Paranaguá (PR), 83255-000, Brasil.
[2]Present address: Centre for Water Research, University of Western Australia, Nedlands, WA 6009, Australia.

SSDI 0025-3227(95)00103-4

Ashley and Zeff, 1988; Ferland, 1985; Finkelstein and Ferland, 1987).

Water circulation and sediment dispersion in coastal lagoons and estuaries are caused by processes varying from density gradients to tides (Kjerfve and Magill, 1989). In embayments with unrestricted tidal flow and insignificant fresh-water inflow, tidal currents generally dominate sediment dispersion. The tidal circulation is a function of the basin hypsometry, i.e., the vertical distribution of basin surface-area, which determines the character of the progressive inundation and subsequent emergence of the intertidal zone during a tidal cycle (Boon and Byrne, 1981). Since propagation of the tidal wave is depth-dependent, the hypsometry affects the overall tidal characteristics (time lag, phase lag, range, asymmetry) and direction of net sediment-transport (Boon and Byrne, 1981; Dronkers, 1986; Friedrichs and Aubrey, 1988). During the sediment infilling of a back-barrier basin, the basin hypsometry inevitably changes, and it is expected that the character of the tidal processes in the basin will alter correspondingly. Basin infilling generally results in an increased proportion of intertidal area, i.e., the ratio of intertidal volume to subtidal volume. This will affect the tidal propagation and may induce changes in the direction of the net sediment transport. In turn, the change in the tidal hydrodynamics and the direction of the net sediment transport modifies the pattern of erosion/deposition within the back-barrier basin.

The mutual interactions between the (tidal) processes and the (basin) morphology form the basis for the morphodynamic approach, as first advocated by Wright and Thom (1977). Only a few investigations have attempted to address the morphodynamic interactions involved in the evolution of barrier estuaries, but have fallen short by failing to provide either: (1) geological evidence of the sedimentation processes (Mota-Oliveira, 1970; Boon and Byrne, 1981) or (2) supportive hydrodynamic data (Roy, 1984; Ashley and Zeff, 1988). It is the aim of this paper to investigate the evolution of a barrier estuary from a morphodynamic perspective, using stratigraphic, morphologic and hydrodynamic evidence from a macrotidal barrier estuary on the central Queensland coast, Australia.

2. Morphologic and hydrodynamic evolution of barrier estuaries

Two opposing conceptual ideas can be applied to explain the evolution of back-barrier depressions: the basin-infilling model of Lucke (1934) and the basin-inundation model of Oertel et al. (1992). The model of Lucke (1934) is conceptualised in Fig. 1A and accounts for marsh development behind a barrier under stationary sea-level conditions through lateral and vertical accretion of the flood-tidal delta(s) and expansion of the margins of the lagoon. As the basin evolves, the surface of the flood-tidal delta connects to the basin's margin and eventually the back-barrier depression becomes infilled. Stratigraphically, the Lucke (1934) model yields an extensive fining-upward sequence, where coarse-grained flood-tidal delta deposits grade into muddy salt-marsh sediments. The model of Oertel et al. (1992) is presented in Fig. 1B and considers the mode of barrier formation of prime importance for the evolution of back-barrier basins. Back-barrier basins may form either by spit progradation or coastal inundation by sea-level rise. According to Oertel et al. (1992), back-barrier basins formed by spit progradation have simple topographies and may evolve into a marsh-filled basin following the model of Lucke (1934). However, embayments that form as a consequence of the inundation of a pre-existing landscape by the sea will inherit the complex hypsometry of former drainage systems (Fig. 1B). During the initial inundation of the basin, the relatively deep drainage channels are separated from each other by pre-Holocene islands and these inter-fluvial areas are transformed into marsh platforms. One inlet will be present at the previous channel axis and is consequently very stable.

In the Lucke (1934) model, the open-water embayment represents the first stage in the evolutionary sequence, whereas the Oertel et al. (1992) model considers the open-water embayment the end-member of the evolutionary cycle. The two opposing models were originally developed for

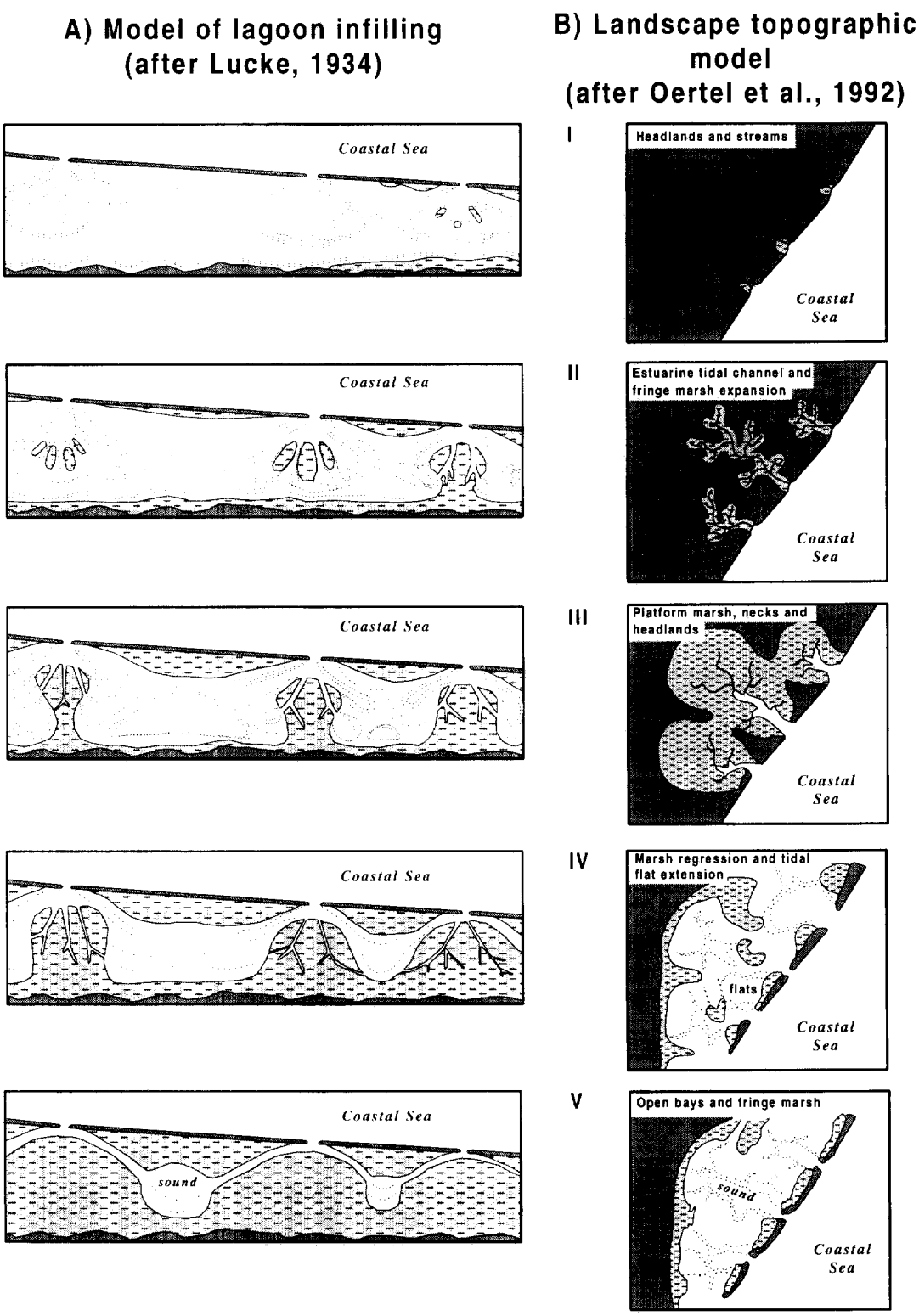

Fig. 1. Schematic models for lagoon evolution (from *I* to *V*) according to (A) the basin-infilling model of Lucke (1934) and (B) the landscape topographic model of Oertel et al. (1992).

areas with different trends in the relative sea level. Whereas the Lucke (1934) model was developed for stationary sea-level conditions, the Oertel et al. (1992) model assumed submergence. For a stationary sea level, the fate of basin evolution typically should be sediment infilling, as suggested by Lucke (1934). Conversely, when the rate of sea-level rise exceeds the rate of basin infilling, an open-water lagoon will eventuate, as predicted by Oertel et al. (1992).

Many researchers have postulated that in shallow estuaries, i.e., estuaries where the channel depth is less than 10 m and the channel length is less than 10 km (Speer and Aubrey, 1985), the net bedload transport direction may change from landward to seaward as a lagoon infills (Mota-Oliveira, 1970; Byrne et al., 1974; Byrne and Boon, 1976; Boon and Byrne, 1981; Friedrichs and Aubrey, 1988; Friedrichs et al., 1992). Three investigations in particular are worth reviewing in this respect, namely those of Boon and Byrne, 1981; Friedrichs and Aubrey (1988), and Friedrichs et al. (1992).

The first direct insight into the effects of sedimentation upon tidal hydrodynamics, and the resulting change from flood- to ebb-dominance, was provided by Boon and Byrne (1981), who investigated the vertical tidal asymmetry for different stages of basin infilling. Their numerical results suggest that during the early stages of basin infilling, the duration of the flooding tide is shorter than that of the ebbing tide. Assuming that the same amount of water passes in either direction during a tidal cycle, the shorter duration of the flooding tide must result in faster velocities and flood-dominant sediment transport. As the basin infills, the duration of the flooding tide becomes progressively longer, ultimately resulting in faster ebb-velocities and ebb-dominant sediment transport. Thus, according to Boon and Byrne (1981), a flood-dominant open basin may change into an ebb-dominant salt-marsh estuary as sedimentation within the basin induces changes in the hypsometry.

Friedrichs and Aubrey (1988) investigated the geometry and the distortion of the vertical tide in 26 tide-dominated estuaries on the East Coast of the USA and compared measured tidal elevations with numerical results. Their results suggest that flood- and ebb-dominance in shallow estuaries can be assessed by considering the relative tidal amplitude in the estuary (ratio of tidal amplitude a to channel depth h) and the relative estuarine intertidal storage (ratio of volume of intertidal storage to volume of the channel at mean sea level). Generally, flood-dominance occurs when the tidal amplitude is large relative to the channel depth, whereas ebb-dominance takes place when the relative intertidal storage is large (see also Aubrey and Speer, 1985). In addition, Friedrichs and Aubrey (1988) point out that the relative tidal amplitude alone may be suffice to dictate overall tidal asymmetry, with deep estuaries (small relative tidal amplitudes) exhibiting ebb-dominance and shallow estuaries (large relative tidal amplitudes) displaying flood-dominance. Friedrichs and Aubrey (1988) further suggest that the effects of tidal distortion on bedload sediment transport is to make shallow systems shallower and deep systems deeper. Consequently, an evolutionary change from flood- to ebb-dominance, as proposed by Boon and Byrne (1981), may only be possible for weakly flood-dominant systems.

Finally, Friedrichs et al. (1992) stressed the importance of strong positive feedback between the initial embayment morphology and the hydrodynamic processes. Based on analytical results and numerical models, Friedrichs et al. (1992) postulated that the velocity asymmetry plays a central role in the origin and maintenance of the back-barrier environment. Shallow basins are associated with small tidal prisms and narrow intertidal areas, and tend to be flood-dominant. Deep basins, on the other hand, are usually characterised by large tidal prisms and wide intertidal areas, and are ebb-dominant. In both cases the velocity pattern reinforces the morphology: flood-dominance enhances landward sediment transport and basin infilling, whereas ebb-dominance enhances seaward sediment transport and channel incision. Thus, flood-dominant systems become progressively shallower and ebb-dominant systems become progressively deeper, in agreement with Friedrichs and Aubrey (1988). The work of Friedrichs et al. (1992) further suggests that if a relatively deep drainage channel is present in the antecedent topography, the back-barrier basin is ebb-dominant throughout its evolu-

tion. If, on the other hand, there is no significant channel present, the basin will remain flood-dominant.

3. Study area

The study area is on the coastline of tropical central Queensland (21°S), southeast of Mackay (Fig. 2). Tides in the area are semi-diurnal and macrotidal, with mean spring tide ranges decreasing from 5.5 m at Hay Point to 4.5 m at Cape Hillsborough (Australian Tide Tables, 1992) (Fig. 2). Waves are locally generated and significant wave heights range from 0.6 to 1.0 m with periods between 5 and 7 s (Beach Protection Authority, 1986). Storm surges are common in this cyclone-prone area, but the elevation of the majority of the storm surges has been less than 0.6 m above predicted water level (Gourlay and Hacker, 1986). The average rainfall in the area is 2100 mm/year and falls predominantly during summer thunderstorms (Bureau of Meteorology, 1965).

Two estuaries were extensively investigated (Eimeo and Louisa Creek; Fig. 2), but this study focuses on the hydrodynamics and stratigraphy of Louisa Creek, a small (3.1 km^2) and shallow bar-

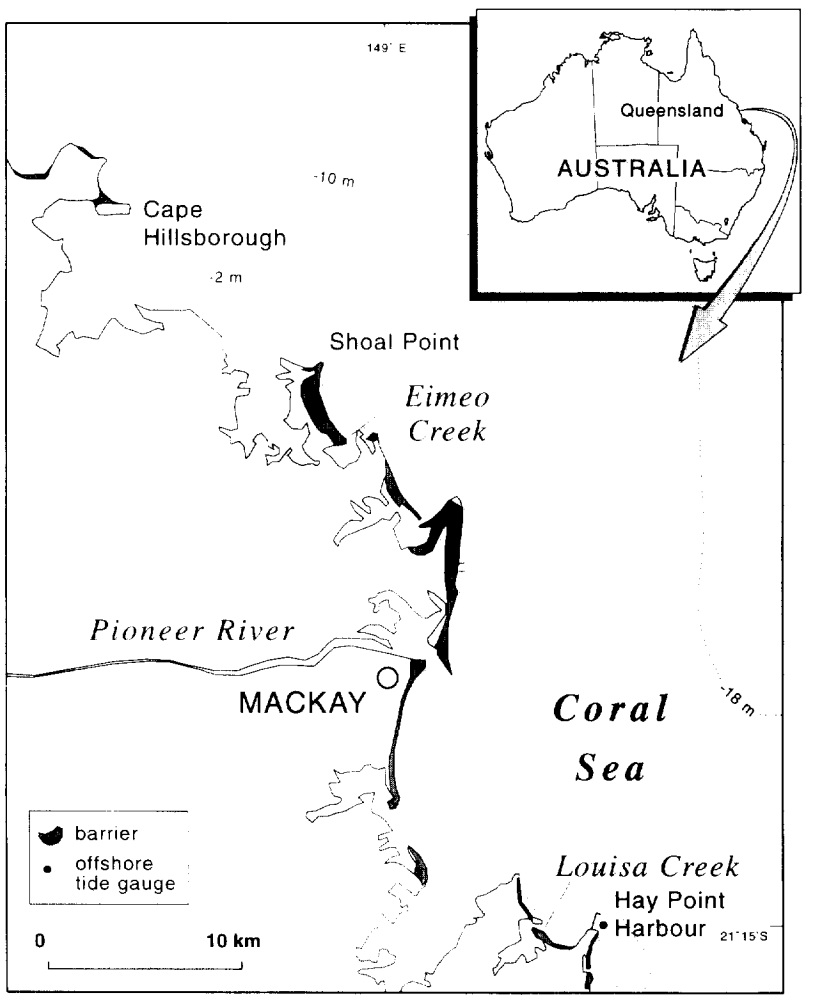

Fig. 2. Location map of the study area. The −2 m isoline is the approximate spring tide low water mark.

rier estuary located southeast of the Pioneer River (Table 1). Louisa Creek is a partially infilled bedrock basin, colonised by mangroves, with one meandering channel connected to the open ocean via a tidal inlet (Fig. 3). The shore inside the estuary is formed by bedrock. A small sandy barrier on the northern side separates the estuary from the sea. The only fresh-water source for the creek is the rainfall-associated run-off from the catchment area (28 km^2). If integrated for 6 hours,

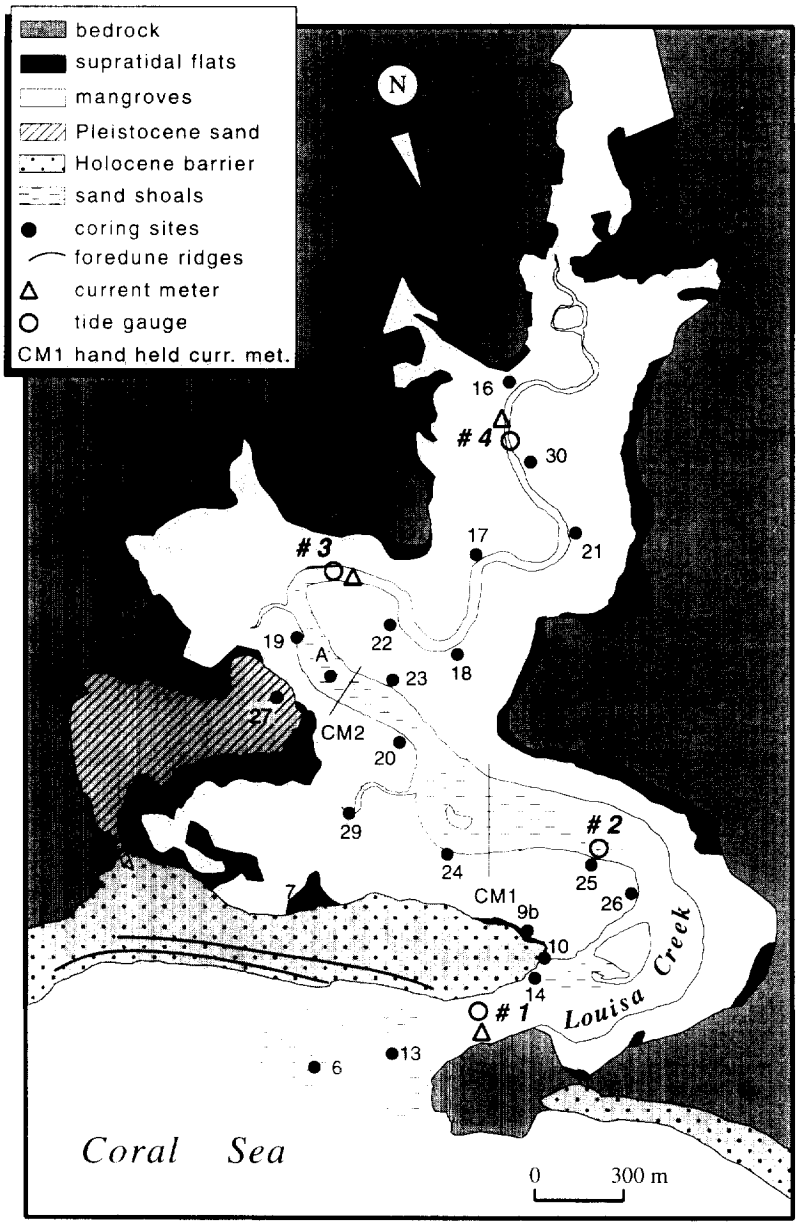

Fig. 3. Surface morphology of Louisa Creek area with locations of the tide gauges, current meters, and coring sites. Question marks show areas where the boundary is uncertain.

Table 1
General characteristics of Louisa Creek

Surface area	km^2	%
Total	3.09	
Mangroves	1.80	58.4
Tidal channels	0.53	18.8
Salt pans	0.70	22.8
Tidal prism	3.5×10^6 m^3	
Offshore tides		
Mean neap range	2.3 m	
Mean spring range	4.9 m	
Maximum spring level	3.8 m AHD	

maximum runoff values represent less than 10% of the month averaged tidal prism, or nearly 30% of the smallest measured tidal prism (Lessa, 1994).

The estuarine channel displays three distinct sections (Figs. 3 and 4): (1) a well-defined and scoured throat, with coarse-grained, carbonate-rich sandy sediments; (2) a wide mid-estuary section with a shallow and irregular thalweg running through shoals composed of medium-sized sand, and (3) an upstream meandering section with a narrow and well-defined channel consisting of a semi-cohesive, poorly sorted sediment. Fig. 4 shows the longitudinal channel profile of the estuary, with the ocean tidal planes, mean low water level inside the estuary and the approximate mangrove-bank elevation. It can be seen that the height of the mangrove banks increases from −0.2 m of the Australian Height Datum (AHD) close to the mouth to +2.2 m AHD at the head of the estuary (the heights upstream from station #3 have been inferred). The maximum elevation of the mangrove banks is around mean spring high water level. The ocean low water level regularly falls below the elevation of the channel bed across the ebb-tidal delta. The latter then acts as a natural sill, resulting in almost perched water levels in the estuary during spring low tides (Fig. 4). Due to the presence of several shallows in the mid-estuary section between stations #2 and #3, the water level in the upper part of the estuary is constantly held high during low tides.

The barrier fronting the estuary (Fig. 3) has undergone transgressive and regressive phases, as indicated by its morphology and stratigraphy (Masselink and Lessa, 1995). The transgression ceased about 6500 yrs B.P. (Hopley, 1983), and thereafter the barrier has prograded approximately 100 m under conditions of a 1.5 to 2 m falling sea

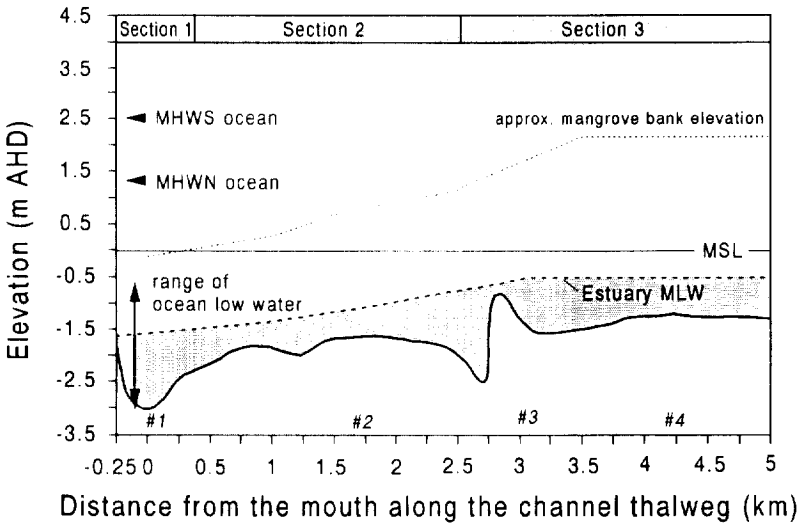

Fig. 4. Longitudinal profile along the thalweg path of Louisa Creek, with the elevation of the main thalweg (thick line) and the estuary mean low water level (dashed line), the approximate elevation of the intertidal mangrove banks, the mean high water level for neap tides (*MHWN*) and spring tides (*MHWS*), and the elevation range of the ocean low water level (vertical arrow). The positions of the measurement stations are also indicated.

level, supplied predominantly by inner shelf sediments (Masselink and Lessa, 1995).

4. Methods

Monitoring of the tidal water motion within the estuary was undertaken for 33 days during February–March 1992, when the highest tides of the year were predicted. Water levels were recorded continuously at all stations (#1, #2, #3 and #4: Fig. 3) with Bristol tide gauges, whereas the ocean tide was recorded 3 km offshore by the Queensland Department of Transport. Current velocities (10 min block-averages) were recorded in the thalweg at 0.5 m from the bed at stations #1, #3 and #4 with Aanderaa current meters. Battery problems with current meters at stations #3 and #4 permitted only two weeks of measurements.

Depth-averaged velocities for stations #1, #3 and #4 were calculated following recommendations by Black and Healy (1986). Shear velocity was approximated using the logarithmic Karman–Prandtl equation for rough turbulent flow (Dyer, 1986). The roughness length at stations #3 and #4 was based on the grain roughness ($z_o = D_{50}$), whereas at station #1 the bedform dimensions were used ($z_o = 0.01$, see Lessa, 1994). Near-bottom sediment transport rates were estimated from the bedload transport formula of Meyer-Peter-Müller with a critical shear stress (in Fry and Aubrey, 1990). It should be pointed out, however, that shear stresses and mean cross-sectional current velocities were based on single-point measurements at each station. Therefore, this is a qualitative, rather than a quantitative, approach.

Sediment cores in the estuary and in the nearshore zone were taken with a mobile pneumatic vibro-core unit (for locations of the cores see Fig. 3). Cores ranging from 2 to 6 m in length were obtained with a stainless steel core barrel 6 m long and 50 mm diameter. At the site, the sample in the core barrel was extruded into plastic sleeves 1 m in length and 65 mm diameter. Although this procedure permits inspection of the core at the site and allows for better planning of the subsequent coring locations, it unfortunately destroys the sedimentary structures in sandy deposits due to the expansion of the sediment core inside the plastic sleeve. One additional core (core *A*—Fig. 3), taken with a punch corer in a previous study, is included in the analysis. The ground levels of the coring sites were determined with a TOPCON total survey station and were corrected to AHD level using established benchmarks.

In the laboratory the cores were cut in 0.5 m lengths, opened with a spoon and subsequently logged. Sub-samples were taken from each identified sedimentary unit for textural analysis. All cores were photographed and, of some of the cores, epoxy resin peels were made for future reference. Sediment samples were analysed with a settling tube for sample sizes under 2 mm and with standard sieving techniques (1/4 phi intervals) for samples with coarser fractions.

5. Results

5.1. Hydrodynamics

A significant variation of the ocean tide range occurred during the measurement period with a maximum spring tide range of 6.7 m and minimum neap tide range of 1.5 m. The variation in the tidal range within the estuary was significantly less, mainly due to the effect of tidal truncation caused by the pooling of the water within the estuary (Fig. 4). The mechanism of tidal truncation is illustrated in Fig. 5, which compares the tidal curves in the ocean and at the mouth of the estuary for different tide ranges. As the tidal range increases progressively from neap to spring tide (Fig. 5a–c), the ocean tide level will eventually fall below the channel elevation across the ebb-tidal delta ($\cong -2$ m HAD; Fig. 4). When this occurs, the water level inside the estuary remains perched, resulting in a reduction of the tidal range. The truncation of the low tide level within the estuary due to the shallowness of the tidal channel across the ebb-tidal delta is directly responsible for the vertical asymmetry of the tide. As the outflow of water during the ebbing tide is retarded due to the almost perched conditions, low water in the estuary increasingly lags behind that of the ocean tide. This results in a tidal asymmetry characterised by

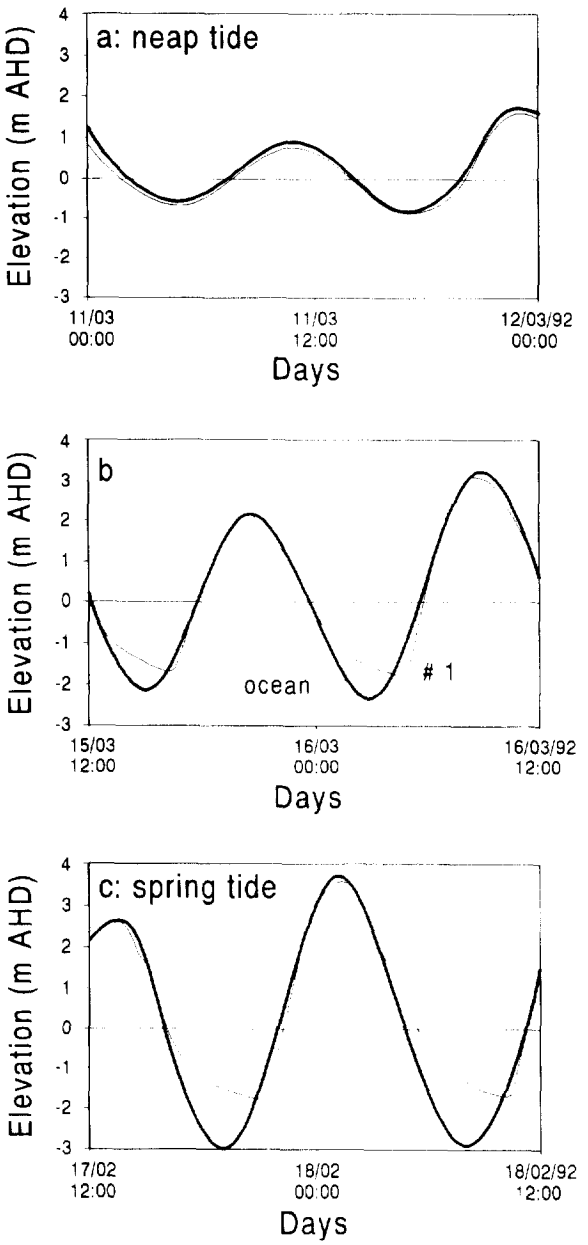

Fig. 5. Tidal curves, representing different tidal range conditions in the ocean and at station #1.

a faster rise and a slower fall of the water level. The tidal asymmetry increases with increasing tide range.

Fig. 6 shows the tidal currents measured in the channel at stations #1 and #4 during spring and

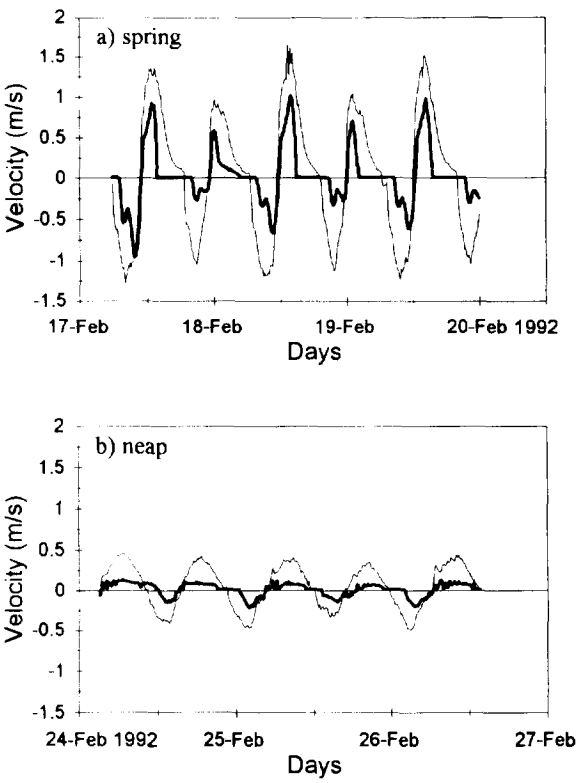

Fig. 6. Spring (a) and neap (b) tidal currents measured 0.5 m above the bed at stations #1 and #4.

neap tides. Due to the large differences in tidal range between spring and neap tides, maximum flow velocities are at least twice as fast during spring tides than during neap tides. During spring tides (Fig. 6a), ebb-velocities are larger than flood-velocities, whereas during neap tides (Fig. 6b), flood-velocities exceed those during ebb. Typically, during spring tides the flood-velocity exhibits two peaks, the first one occurring before mid-tide and the second one just prior to high tide. The first flood-velocity peak is associated with a steep pressure gradient created by the fast rising tide in the ocean and a slower rising tide in the estuary (Dronkers, 1986; Lessa, 1994). The second flood-velocity peak is associated with the swift inundation of the high-intertidal mangrove area, resulting in a sudden increase of the discharge, thereby forcing higher flood-velocities along the channel (see also French and Stoddart, 1992).

Except during the smallest neap tides, the verti-

cal tidal motion in the estuary is characterised by a faster rise and a slower fall of the water level (Fig. 5). Therefore, a flood-dominance of the tidal currents is anticipated. Fig. 7 shows the natural logarithm of the ratio of maximum ebb- over maximum flood-velocity for each tidal cycle, plotted against ocean high tide level. The logarithmic representation was chosen as it distributes ratios larger (stronger flood) and smaller (stronger ebb) than 1 into negative and positive values, facilitating the graphical interpretation. During spring tides, the mangrove areas are inundated and drainage during the falling tide is impaired by the shallow water depths and the presence of dense vegetation. Consequently, the rate of the falling tide within the estuary is reduced with respect to that of the ocean, resulting in a relatively steep hydraulic gradient and large ebb-velocities (see also French and Stoddart, 1992). Therefore, during spring tides, ebb-velocities greatly exceed flood-velocities (Fig. 7). The steepness of the hydraulic gradient, and thus the ebb-velocity, is proportional to the relative extent of the mangrove area (see also Friedrichs and Aubrey, 1988), which in turn depends on the longitudinal position within the estuary and the ocean high tide level. The level of the ocean high tide, required to trigger faster ebb-velocities is about +3.2 m AHD at station #1 and +2.5 m AHD at stations #3 and #4 (Fig. 7). The difference is ascribed to the smaller mangrove area close to the mouth.

Fig. 8 shows the estimated net sediment flux per

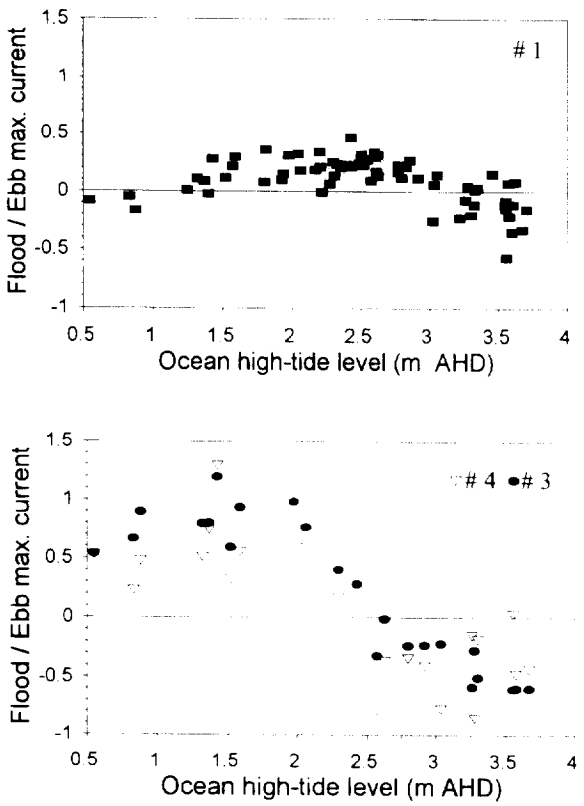

Fig. 7. Natural logarithm of the ratio of maximum flood-to-ebb currents during each tidal cycle compared to the corresponding ocean high tide level. A value of 0.69 (−0.69) is equivalent to ebb (flood) currents twice as strong as flood (ebb) currents.

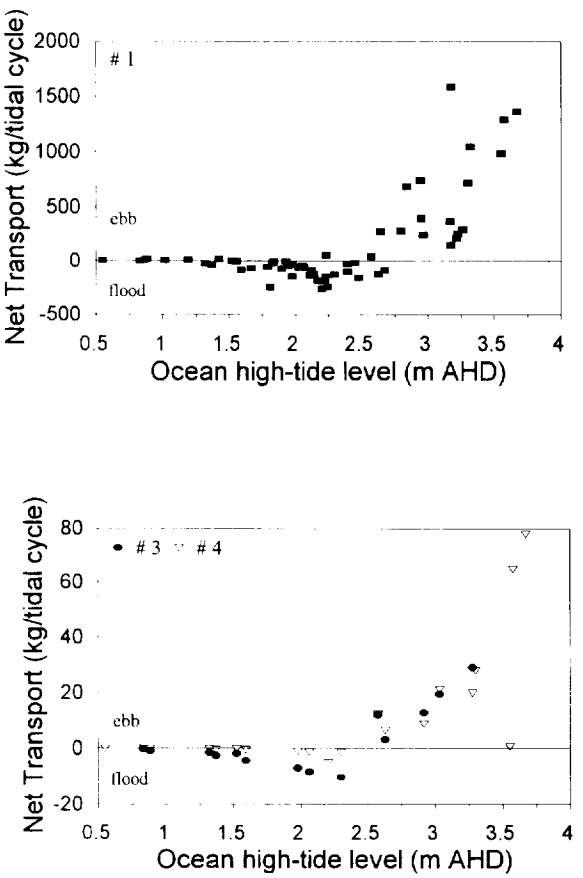

Fig. 8. Net sediment transport (in kg/tidal cycle) compared to the ocean high tide level for individual tidal cycles at stations #1, #3 and #4, based on the sediment transport equation of Meyer-Peter and Muller (in Fry and Aubrey, 1990).

tidal cycle as a function of tide range. Because the channel bed at stations 3 and 4 consists of consolidated muddy material, *potential* rather than *actual* sediment transport volumes were estimated at these stations. During spring tidal cycles, net potential sediment flux is ebb-directed for all stations and considerably exceeds sediment fluxes occurring during neap tides. During neap and intermediate tidal cycles, net potential sediment flux is flood-directed. The amount of potential sediment transport at the mouth of the inlet is two orders of magnitude larger than at any of the inland stations. The level of the ocean high tide, required to trigger a net potential ebb-directed sediment flux is approximately +2.5 m AHD (Fig. 8).

To determine the annual net sediment flux, the frequency-distribution of the tidal elevations should be taken into account. For the data collected at station #1 (Fig. 8a), a curve was fitted that expresses the volume and direction of potential sediment flux as a function of the ocean high tide level ($R^2 = 0.6$; Lessa, 1994). Subsequently, the expression of the curve and the frequency-distribution of high tide elevations for 1992 were used to compute the net annual potential sediment flux. The results show an ebb-dominance of the thalweg, which may correspond to a net seaward-directed sediment flux in the order of 10^2 m^3/year.

It is concluded from the hydrodynamical measurements and the sediment transport estimates, that the channel cross-sections at stations #1, #3 and #4 present a long-term ebb-dominance and that no sediments from the nearshore zone enter the estuary. Unfortunately, it is not possible to determine the overall net-direction of sediment transport in the mid-estuary sections (between station #1 and #3), because local areas of flood- and ebb-dominance coexist in the shoals (see also Friedrichs et al., 1992). The channel bed at the upstream section (stations #3 and #4) consists predominantly of consolidated material, and the ebb-dominant flow at this location is not expected to transport large quantities of sediment into the mid-estuary section. Therefore, a balance between flood- and ebb-directed sediment transport is inferred for the mid-estuary section (Lessa, 1994).

In summary, the hydrodynamics within the estuary are controlled by the depth of the channel bed across the ebb tidal delta ($\cong -2$ m AHD) and the elevation of the mangrove banks along the channels ($\cong +2$ m AHD). The former influences the propagation of the tidal wave, whereas the latter plays a role in determining whether maximum current velocities are attained during the ebbing or flooding tide. In general, the estuary can be considered ebb-dominant.

5.2. Lithofacies

On the basis of texture, colour, elevation and contact, nine lithofacies were identified in the estuary (Fig. 9). Three of these are tentatively interpreted as pre-Holocene, whereas the remaining are regarded as Holocene. From older to younger, the lithofacies can be described as:

Facies 1

Pleistocene congl: a very cohesive, very poorly sorted, red/orange conglomerate (pebbles–sand) embedded in a clayey matrix was at the bottom of cores #17, #22, #23, #25, #26 and #28 (Fig. 9). The unit crops out along the west margin of the channel from the mouth of the estuary to core #25 and in parts of the deep meandering channel upstream from core #19. In addition, the surface of the supratidal zone at the head of the estuary (Fig. 3) is formed by this unit. The unit has about 6 m relief and the minimum elevation of its surface follows the longitudinal axis of the estuary. This is evidence that the unit makes a seaward-sloping paleovalley beneath the present estuary. The unit is interpreted as the landward extension of the regional sub-surface reflector of pre-Holocene age present on the inner shelf (Hegarty, 1983).

Facies 2

Pleistocene estuarine mud: a very cohesive, light grey mud, with restricted areal extent was in core #30 (Fig. 9) and crops out locally along the east margin of the channel upstream of core #19. The facies is approximately 0.5 m thick and lies unconformably over Facies 1. It is tentatively interpreted as a Pleistocene estuarine sequence.

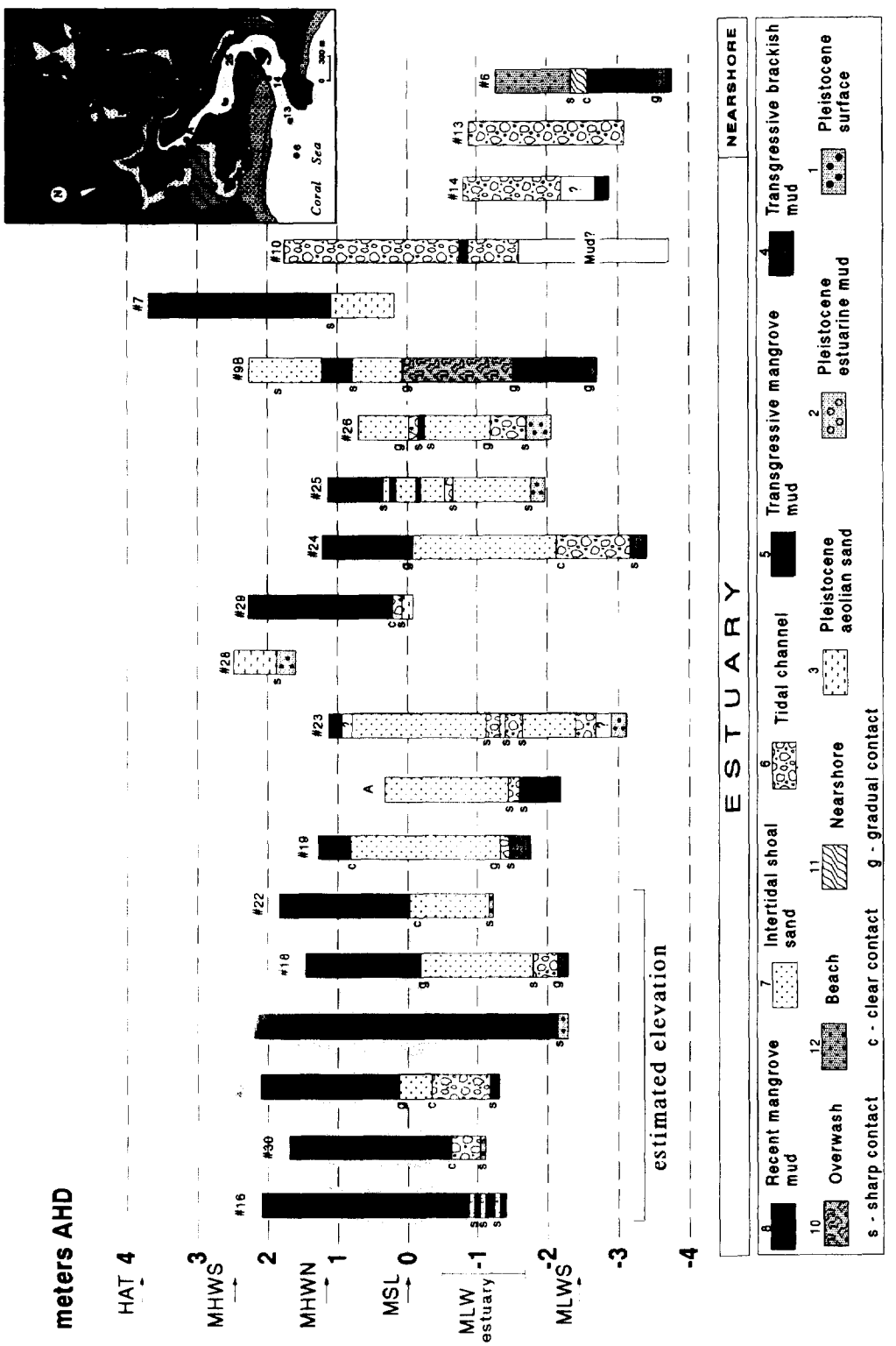

Fig. 9. Sediment cores and interpreted sedimentary facies obtained in Louisa Creek and the nearshore area, with their respective elevations in meters AHD. Tidal planes for Hay Point Harbour (about 3 km offshore) is shown on the *y*-axis (*HAT* = highest astronomical tide).

Facies 3

Pleistocene aeolian sand: a very fine, very well-sorted white sand, locally mottled in green or orange and composed entirely of quartz. It overlies the Pleistocene surface (#28) and underlies recent estuarine mud (#7) and tidal channel sands (#29) (Fig. 9). Morphologically, the unit is a supratidal feature of the back-barrier (Fig. 3) and it reaches a thickness of at least 2 m. The erosive nature of the contact with overlying units suggests that part of this facies has been eroded. Based on the sediment characteristics, the elevation at which the unit occurs and the laterally discontinuous nature, this facies has been interpreted as a Pleistocene aeolian sand sheet, possibly associated with the last interglacial period.

Facies 4

Transgressive upper-intertidal mud: a semi-cohesive, light to dark grey sandy mud, with minor colour variation associated with the organic content. This unit was at the bottom of the estuarine cores #21, #18, #19, #20, #24 and #9b and beach/nearshore core #6 (Fig. 9). The unit is always found at subtidal elevations and its thickness is unknown. However, sharp contacts with overlying sandy units suggest that part of the deposit has been eroded. The unit is interpreted as a Holocene upper-intertidal swamp deposit, associated with the initial inundation of the antecedent topography as sea level rose. A wood fragment collected at -1.85 m AHD from a similar stratigraphic location in the other studied estuary was carbon dated (SUA #3077) at 7,800 years B.P (Lessa, 1994).

Facies 5

Transgressive mangrove mud: a soft, organic-rich and dark brown mud, with rare sand laminations. The unit overlies the transgressive upper-intertidal mud with a gradual contact and was found in the estuarine cores A and 9b, and in the lower-intertidal core #6 (Fig. 9). Upper contacts are sharp with either tidal channel or intertidal shoal deposits, evidence that lowering of the surface may have occurred. The cored thickness of the facies was less than 1 m and the maximum elevation is intertidal (-1.5 m AHD). Due to its texture and the large amount of organic material, the deposit is interpreted as an estuarine mangrove deposit, formed during the Holocene transgression.

Facies 6

Subtidal channel sand: a yellow, coarse to very coarse grained, poorly sorted sand, showing varying amounts of shell fragments and dark grey mud balls. The unit was in all the estuarine cores except cores #17, #22 and #9b (Fig. 9). This facies frequently fines upward, grading into intertidal shoal sand. However, clear contacts with overlying recent mangrove deposits were also apparent, specifically in the upper reaches of the estuary (#30 and #29). The lower contact is represented by an unconformity with transgressive upper-intertidal mud in cores #21, #18, #19, #20 and #24. The thickness of the unit varies from a centimetre thick (cores #16, #19, #20, #29, #25 and #26) to more than 1 m (cores #24, #10, #14 and #13). The elevation of the unit varies widely, but is always below mean sea level (MSL $\cong 0$ m AHD) except for core #29 and #10. The unit is interpreted as subtidal channel deposits, excluding the occurrence in core #10, which appears to be part of a flood-tidal delta.

Facies 7

Intertidal shoal sand: a fine to medium grained, well-sorted, yellow to light grey sand, with small amounts of heavy minerals and sparse concentrations of shell fragments and pieces of mangrove wood few centimeters thick. The unit was almost everywhere in the estuary north of core #30, in cores #21, #18, #22, #19, A, #23, #20, #24, #25, #26 and #9b (Fig. 9). The lower and upper contacts of this facies are commonly gradational, overlying subtidal channel deposits and underlying recent mangrove mud. The facies forms a wedge, and at least in the upper half of the estuary it thickens seaward to about 3.5 m in core #23. The elevation is intertidal, restricted between -2.5 m and $+1.5$ m AHD. This unit is interpreted as low-intertidal shoal sand deposits.

Facies 8

Recent mangrove mud: a soft, dark and organic-rich mangrove mud, at the surface of most cores

(Fig. 9). Thin sand laminations (1–2 cm) are common, increasing in number in the downstream direction and also with depth. Due to the seaward increase in the elevation of the underlying intertidal shoal sand, the thickness of the mud generally decreases from more than 3 m upstream to less than 0.5 m close to the inlet. The maximum elevation of this facies is about +2.2 m AHD (core #29), which is close to mean high water spring tide level (MHWS). The unit is interpreted as recent mangrove mud.

Facies 9

Washover deposit: a medium grained sand to gravel was identified only in core #9b (Fig. 9). Core #9b was taken just behind a scarp at the back of the barrier close to the mouth of the estuary (Fig. 3) and the identified unit was composed of successive layers of sand and pebbles. The unit overlies transgressive mangrove mud with a gradual contact and is interpreted as a washover deposit.

The overall stratigraphic profile is characterised by a seaward-thickening wedge of sand embedded in muddy sediments, extending along the seaward three quarters of the estuary (Fig. 10). The stratigraphy reveals a transgressive and a regressive sequence. The transgressive sequence is restricted to the first 1 m of the stratigraphic section, where upper-intertidal and mangrove mud deposits are overlaid by tidal channel and intertidal shoal facies. The regressive sequence is characterised by a general fining upward sequence up to 5 m thick, that culminates with mangrove mud.

6. Evolutionary history

Louisa Creek has evolved from a partially open ≅6 m deep depression into a nearly mangrove-filled barrier estuary, where channels account for 19% of the present estuarine area. Because no significant amounts of freshwater enters the estuary, the Holocene sediments contained within the estuary are derived from the sea and in-situ biogenic production.

Considering the extensive subtidal channel sand deposits (Facies 6) in the estuary (Figs. 9 and 10), tidal currents must have played a significant role in the early stages of estuarine sedimentation. Part of the sediment comprising the tidal channel sands probably was derived from Facies 1 and conveyed up the channel by flood tidal currents. In addition, tidal currents have eroded transgressive mud deposits (Facies 4 and 5), as indicated by unconformities at the top of these facies and the presence of dark grey mud balls within the subtidal channel sediments. The ephemeral streams draining the watershed may also have provided some of the sediment contained within the subtidal channel deposit, especially at the head of the estuary.

Bed aggradation allowed for a gradual transition from subtidal channel sand (Facies 6) into intertidal shoal sand (Facies 7). Intertidal sand shoals developed along the lower two thirds of the estuary, with the landward limit just upstream of core #21 (Figs. 9 and 10). The presence of mangrove wood fragments within the intertidal shoal sand deposits indicate that, during the bed aggradation phase, mangroves existed along the margins and in the upper region of the estuary.

Following the deposition of intertidal shoal sands, mangrove mud (Facies 9), which was already accumulating in the distal part of the estuary, prograded over the lower intertidal sand shoals. The lower part of the mangrove mud facies is characterised by sand laminations. The thickness and the number of laminations decreases upward and indicate a gradual reduction of the current energy level during mud deposition. The surface of the mangrove mud at the head of the estuary has reached an elevation near mean spring high water. The mud surface near the mouth of estuary, however, is almost 1 m lower, suggesting that the mangroves are prograding seawards and that the estuary is still infilling.

In the upper reaches of the estuary, intertidal shoal sands underlie the recent mangrove mud (Fig. 10). This implies that the well-incised tidal channels that are now found in the upper part of the estuary have evolved from a morphology similar to that presently observed in the mid-estuary section, characterised by wide and shallow channels and intertidal sand shoals. Thus, as sedimentation built up the intertidal area, scouring and deepening of the bed occurred and the wide and

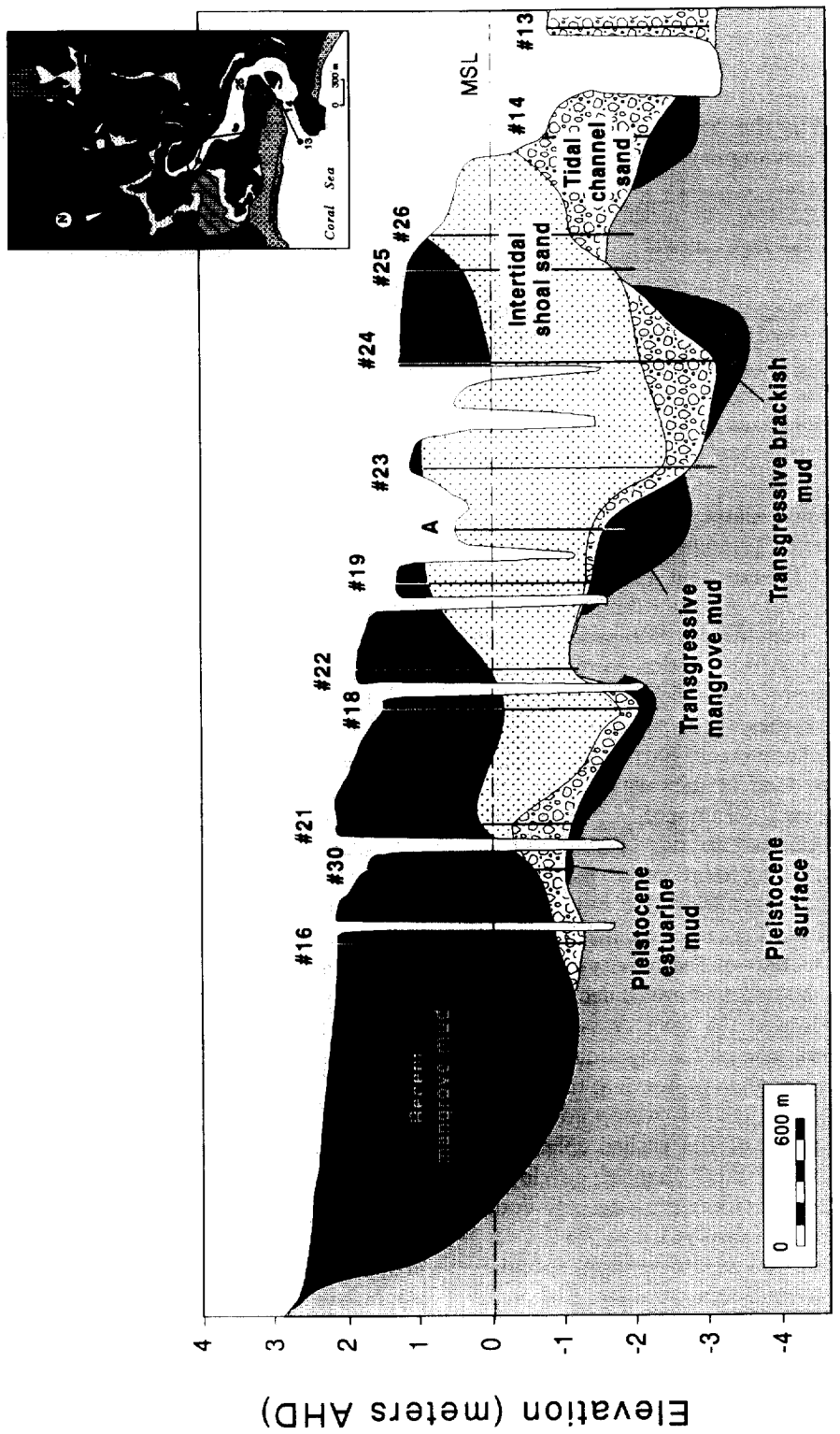

Fig. 10. Longitudinal stratigraphic profile of Louisa Creek showing the 2-D geometry of the identified sedimentary facies.

shallow channel(s) became progressively narrower and deeper. It is suggested that channel incision originated close to the head of the estuary, and subsequently propagated in the downstream direction, as suggested by the downstream decrease in the elevation of the mangrove banks (Fig. 10).

7. Reconstruction and facies model

Fig. 11 shows the reconstructed morphological changes undergone by the estuary in the last 8500 years. As sea level first inundated the present position of Louisa Creek (Fig. 11a), an open lagoon formed behind two headland-attached barriers. The lagoon probably was connected to the ocean by a flood-dominant tidal inlet. The rate of sea-level rise was approximately 4 mm/year (Thom and Roy, 1983) and, assuming an average mud deposition rate of 0.5 mm/year (Nichols, 1989), grossly exceeded the rate of lagoon-infilling. Under these conditions, mangrove colonisation might have been restricted. As inundation continued and the paleovalley began to be flooded, an upper-intertidal swamp (Facies 4) formed, following the course of the ephemeral creek. Farther inland, the Pleistocene aeolian sand (Facies 3) was incorporated into the lagoon environment.

As sea level continued to rise (Fig. 11b), the western side of the lagoonal shore backed up against the hill slopes, resulting in a reduction of the landward translation rate of the lagoonal shoreline relative to that of the barrier shoreline. Consequently, the lagoon narrowed, decreased its tidal prism and reduced the inlet cross-sectional area. On the eastern side of the lagoonal system, the ongoing transgression kept flooding the paleovalley and the upper-intertidal swamp continued migrating up the path of the earlier ephemeral fresh-water streams. A tidal channel developed along the axis of the antecedent drainage and flood tidal sand started to be conveyed into the system. Due to the effect of flow channelisation, subtidal channel deposits became more extensive. Although the rate of sea-level rise still exceeded the sedimentation rate, mangroves established at the channel fringes. The Pleistocene aeolian sand was continually incorporated into the lagoonal environment and may have been reworked by tidal currents inside the estuary and by nearshore processes on the shoreface.

At the end of the post-glacial sea-level rise ($\cong$6500 yrs B.P), the western part of the sand barrier attached to another headland, thereby sectioning the previous system into two smaller estuaries (Fig. 11c). A small lagoon formed at the western side, probably without a connection to the sea, and Louisa Creek started to take on its present configuration. Under the influence of a still flood-dominated inlet, a recurved spit began to shape the protuberance observed at the western end of the barrier today. Upper-intertidal swamps became restricted to the head of the estuary and mangroves may have formed a continuous strip of vegetation from the back of the barrier to the head of the estuary. Mud was deposited in the mangrove areas, in particular in the distal parts of the estuary where tidal currents were weaker. Flood tidal deposits advanced landward along the incised paleovalley and coarse sands became deposited at subtidal elevations.

At about 4000 yrs B.P. (Fig. 11d), sea level had fallen approximately 1.5 m relative to that at 6500 yrs B.P., but increasing tidal ranges may have reduced the effects of the regression (Masselink and Lessa, 1995). The estuarine area was maintained, but it is likely that the inundation frequency of high intertidal areas was reduced, resulting in the formation of hypersaline supratidal areas. The fall in sea level, concurrent with onshore and longshore sediment transport, promoted barrier progradation (Masselink and Lessa, 1995). Although the fall in sea level may not have greatly affected the tidal prism, sedimentation and mangrove expansion reduced the estuarine volume. Consequently, inlet cross-sectional area was reduced and the barrier expanded laterally under the influence of the littoral drift (Fig. 11d). The reduction of the tidal prism also decreased the tidal current transport capacity, which lessened the sediment volume entering the estuary. Channel aggradation upstream also aided in lessening the current energy, and coarse channel sediments were covered by intertidal shoal sands. The upper-intertidal swamp remained restricted to local fresh water sources, while the mangroves expanded from

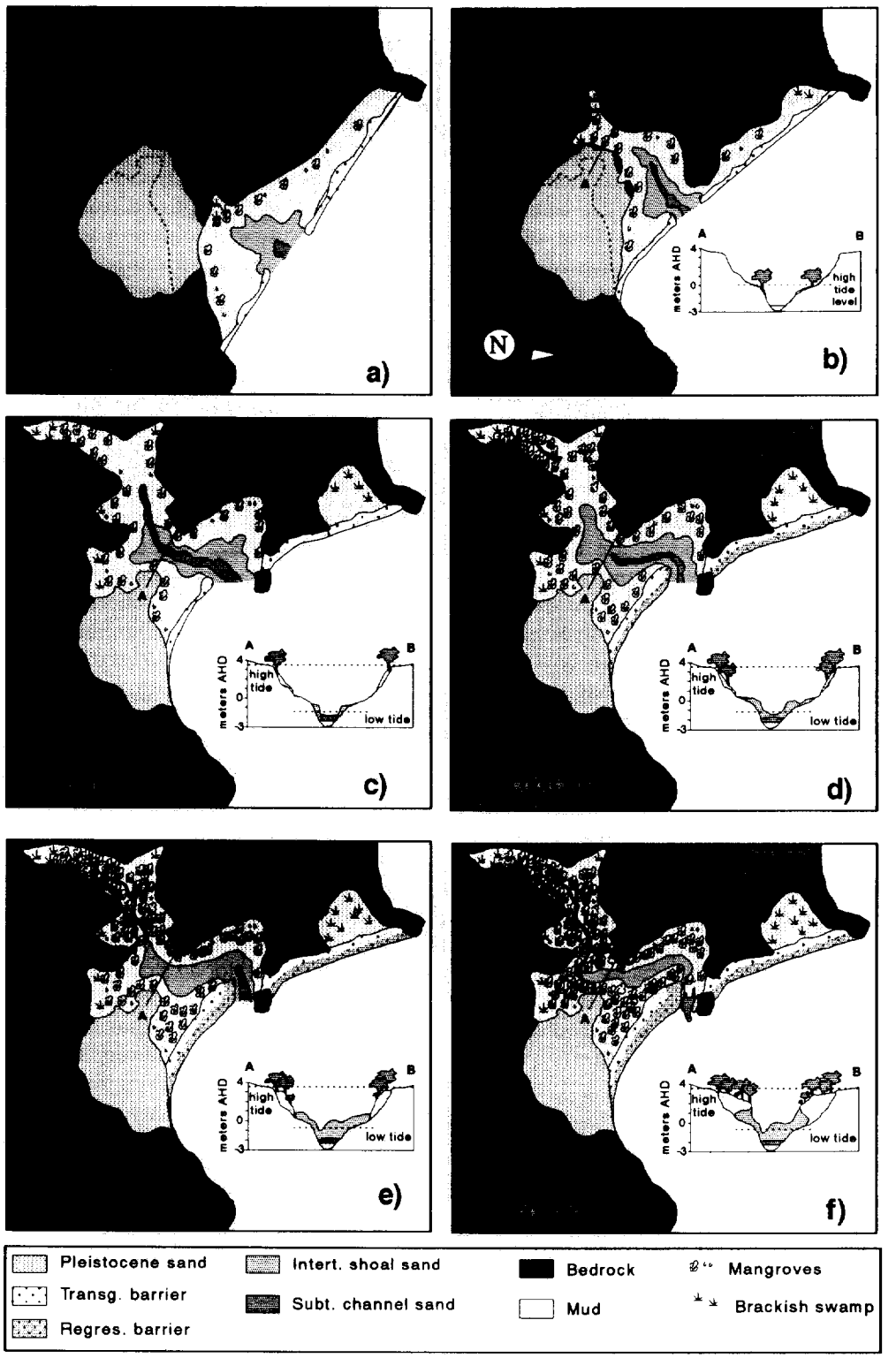

Fig. 11. Evolutionary stages of Louisa Creek from 8500 yrs B.P. (MSL = −6.5 m) (a) until the present (f). The insets show the infilling stages of a section across the paleovalley.

the head seaward and from the sides to the centre. Ample mangrove areas close to the head of the estuary increased the intertidal water storage volume and initiated an ebb-dominated channel along the axis of the previous fresh-water creek.

Estuary evolution in the last 4000 years is shown in Fig. 11e and f. The trends initiated in the preceding stage persisted, namely the sedimentation of the intertidal shoal sands over subtidal channel deposits, the process of mangrove expansion, and the seaward extension of the incised, sediment-deprived channel. More recently, the flood dominance at the inlet has been changed into ebb-dominance, and consequently no sediment enters the estuary from the nearshore.

Fig. 12 shows four schematic cross-sections; one longitudinal and three normal to the axis of the estuary. Fig. 12A and B represent an incised channel and a shoal dominated section, respectively. It is noted that the mud deposits are thicker and occur at higher elevations in the upstream section, whereas the intertidal shoal deposits are thicker at the downstream section. Fig. 12C demonstrates the arrangement of the estuarine facies behind and under the barrier and indicates that the entire barrier is underlain by transgressive mangrove mud and subtidal channel sand (see also Masselink and Lessa, 1995). Finally, a schematic longitudinal facies arrangement is given in Fig. 12D. A continuous layer of upper-intertidal mud (Facies 4) underlies the Holocene sedimentation and the upper-intertidal mud is followed by a seaward-thickening wedge of subtidal-channel sands (Facies 6) and intertidal shoal sands (Facies 7). The top of the intertidal shoal sand facies increases in elevation toward the mouth of the estuary. The top of the mangrove mud layer, on the other hand, decreases in elevation toward the sea.

8. Discussion

8.1. Estuarine evolution

Although the estuarine infilling sequence represents a fining-upward trend, there is a major difference between the manner in which Louisa Creek has evolved and that predicted by the model of Lucke (1934; Fig. 1A) or its improvement by Ashley and Zeff (1988). According to the latter, tidal deltas grow in the landward direction as subtidal and intertidal features, with colonisation of the intertidal areas by salt-marshes. Marsh surfaces close to the inlet will be older and more elevated than those upstream. In contrast, infilling in Louisa Creek progressed from the head of the estuary in a seaward direction and was not significantly aided by an inward-growing flood tidal delta. Consequently, a decrease in the mangrove surface elevation is observed in the seaward direction (Fig. 4).

The initial development of Louisa Creek could have been analogous to the processes operating nowadays in structurally controlled, narrow estuaries with transgressing sea (Boyd and Honig, 1992). The inundation occurred along an incised valley and marine sand was transported approximately 2 km upstream by flood tidal currents. The course of inundation was similar to that proposed by Oertel et al. (1992), where the tidal channel develops along the axis of an antecedent drainage system, with intertidal vegetation occupying the margins of the flooding valley. In addition, Pleistocene estuarine sequences, such as the Pleistocene estuarine mud (Facies 3), limited the total thickness of the Holocene deposition in some places.

8.2. Morphodynamic changes

A major characteristic of the tidal currents in the shallow estuaries in this area appears to be the existence of two flood velocity peaks during spring tides, one in the early stages of the rising tide and the other close to high tide (Lessa, 1994). The second peak occurs following the inundation of the mangroves, which slows down the rate of the rising tide inside the estuary and induces a steepening of the onshore-directed hydraulic gradient. The presence or absence of the second velocity peak had great implications for the morphodynamic development of the estuary. When maximum flood-tidal current velocities occur only at the beginning of the rising tide, deposition of sandy sediments in the intertidal area can only take place at lower intertidal elevations. However, when max-

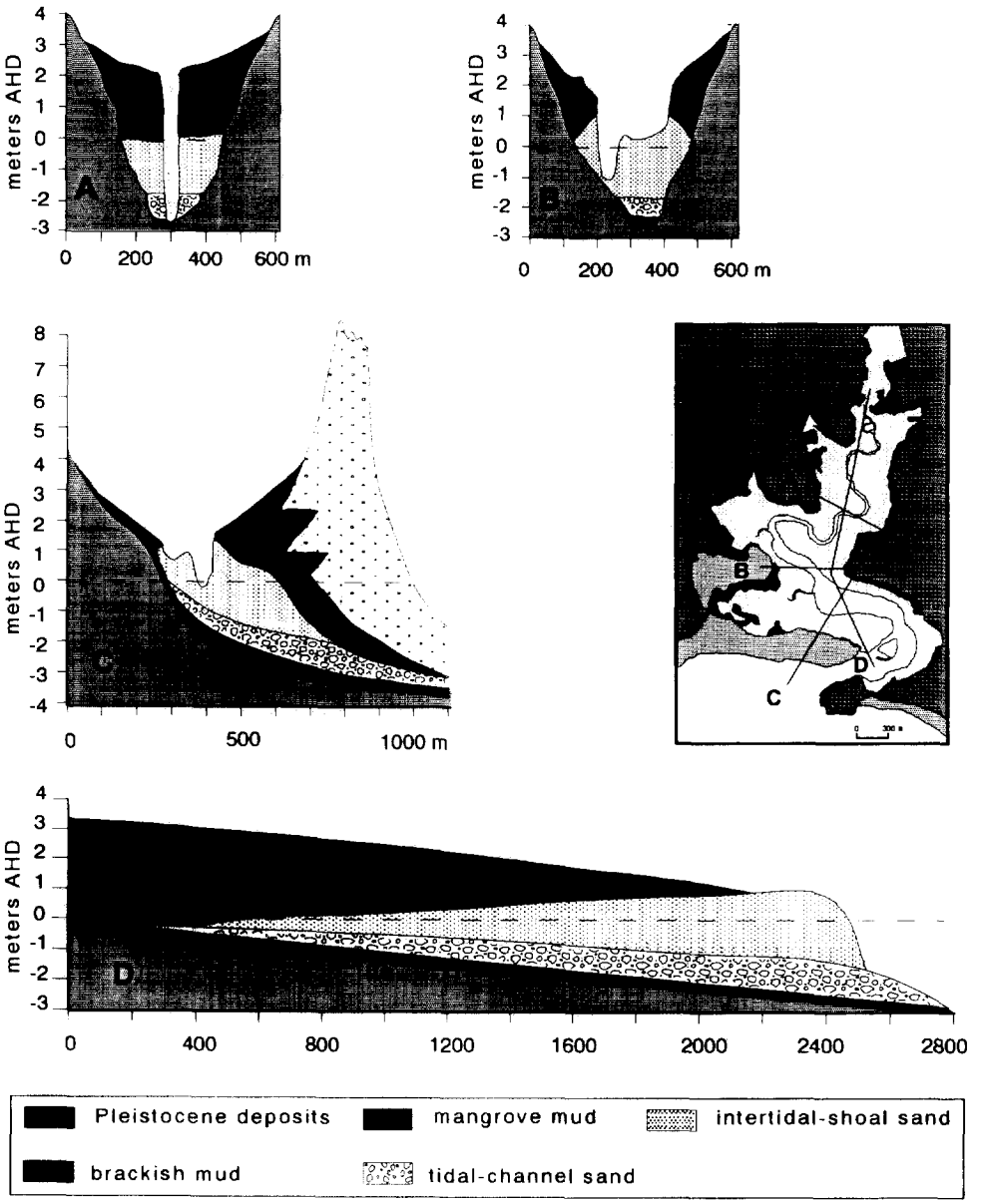

Fig. 12. Schematic stratigraphic cross-sections normal and longitudinal to the main estuary axis.

imum flood-tidal current velocities occur close to high tide, due to the presence of a second flood-velocity peak, sandy sediments can be deposited at considerably higher elevations.

It was observed that the intertidal shoal facies exhibits an overall wedge shape, thickening in the seaward direction (Fig. 12D). The elevation of the upper surface of the intertidal-shoal sands is approximately 0 m AHD ($\cong$MSL) in the upstream cores (#21, #18 and #22), but increases up to 1 m AHD in the cores along the mid-estuary section (#19, #23, #25 and #26) (Figs. 9 and 10). The higher elevation of the intertidal-shoal sand facies at the downstream end of the estuary suggests the

occurrence of relatively large current velocities close to high tide level, which can be ascribed to the second flood-velocity peak. It is therefore inferred that the second flood-velocity peak is a relatively recent phenomenon that has only come about during the later stages of estuarine evolution, after the establishment of an extensive mangrove area.

The present current velocity pattern and ebb-dominant sediment transport are not in accordance with the expected flood-tidal dominance necessary to supply the large volumes of tidal channel and intertidal shoal sands existent inside the estuary. Thus, a change in the direction of the net sediment flux from flood to ebb must have occurred in the late Holocene. The observed positive asymmetry of the vertical tide is contrary to what is expected for established relationships between current-dominance and tidal asymmetry (Boon and Byrne, 1981; Aubrey and Speer, 1985; Speer and Aubrey, 1985; Dronkers, 1986; Friedrichs and Aubrey, 1988; Fry and Aubrey, 1990; Friedrichs et al., 1992). Lessa (1994) suggested that the reason for this discrepancy lies within the elevated high intertidal mangrove area, which only becomes inundated during later stages of the rising tide. This allows only minimal time for reshaping the tidal wave.

The notion that the tidal-wave shape is an indication of flood- or ebb-current dominance led Friedrichs and Aubrey (1988) to postulate that only weakly flood-dominated tidal channels could allow for a transition from flood to ebb dominance. The requirement is that the infilling of the estuary does not decrease channel depth, but only raises the intertidal area at the margins of the tidal basin. This idea partially accounts for the positive feedback between dynamics and embayment morphology (Friedrichs et al., 1992), because strong flood-dominant systems would tend to reduce channel depths, make channel and intertidal areas less distinct, and increase flood dominance even more. It is probable that the vertical tide in Louisa Creek has always been characterised by strong positive asymmetries, because channel depth has always been restricted by the shallow Pleistocene surface (Facies 1). Nevertheless, the advance of the mangroves at the distal part of the estuary promoted the development of dominant ebb-currents during spring tides over major areas of the system.

8.3. Future trends

Presently, in the mid-estuary section of Louisa Creek, the following processes take place: (1) deepening of the tidal channel; (2) vertical accretion on the mangrove banks; (3) lateral mangrove expansion across the intertidal sand shoals, and (4) vertical accretion of the intertidal sand shoals. An interesting question may be formulated as to how the estuary will evolve in the future under the influence of an ebb-dominant or steady-state inlet.

Measurements conducted with hand-held ducted flow meters (Fig. 2) showed that the thalweg along the mid-estuary section is always flood-dominant (Lessa, 1994), and function as a conduit for headward transport of sediments. The sediments can only be carried in the landward direction until the upstream end of the mid-estuary section. There, the flow in the ebb-dominant and well-defined tidal channels flush the sediments back over the shoals. The convergence of ebb- and flood-dominant sediment transport provides conditions for sedimentation and vertical shoal accretion of the low intertidal zone. Fast flow velocities close to high tide, due to the second flood-velocity peak, aids in the elevation of the intertidal area, because sandy sediments can be lifted higher in the water column and deposited on higher elevations. Eventually, the shoals become prone to mangrove colonisation, resulting in channel narrowing and channelisation of the ebb flow at an earlier stage of the falling tide. When maximum spring ebb-currents develop, the flow will be retained within a smaller cross-sectional area, enabling scouring and consequent deepening of the channel to occur.

The proposed model of channel evolution is based on sediment remobilisation in the sandy shoal section of the estuary. Provided there is sufficient sediment stored in the sand shoals, the estuary can continue its evolutionary path—scouring of the tidal channel, building up of the intertidal shoals and expansion of the high intertidal mangrove area—under closed-system conditions by means of sediment recirculation. Sediment budget calculations were performed to determine

whether the volume of sand necessary to build up the intertidal shoal area to +1 m AHD (level of mangrove colonisation) can be made available by the deepening and narrowing of the channel within the mid-estuary section. Least squares analysis was performed to express the channel width as an exponential function of distance along the channel axis (Myrick and Leopold, 1963; Ippen and Harleman, 1966; Wright et al., 1973; Pethick, 1991) using data from the upper half of the estuary ($R^2 \cong 0.7$). The resulting regression line was used to determine the probable channel width in the sand shoal area. The volume of sand that can be made available by channel development and that necessary to raise the shoals to +1 m AHD are 1.4×10^5 m^3 and 1.0×10^5 m^3, respectively. This suggests that Louisa Creek can evolve into an infilled feature without further source of sediment.

9. Conclusions

The study investigates the morphological and hydrodynamical evolution of a macrotidal barrier estuary in an advanced stage of infilling. The tidal wave in the estuary is asymmetric, with the rising tide shorter than the falling tide, and modulated by the degree of tidal truncation at the inlet. At spring tides, enhanced tidal truncation increases the asymmetry, by shortening the rising tide while extending the falling tide. During neap and mean tides, flood-tidal currents are stronger than ebb-tidal currents. However, during spring high tides, a larger volume of water is retained within the mangroves, and stronger ebb flows are generated. Generally, the observed vertical tidal asymmetry is associated with flood-dominant systems, which is contrary to the ebb-orientated long-term net-sediment flux at the inlet.

Three major modern depositional environments were identified: tidal channels, intertidal shoals and a high intertidal mangrove area. The overall stratigraphic profile of the estuary is characterised by a seaward-thickening wedge of sand embedded in muddy sediments, and consists of a transgressive sequence overlain by a regressive sequence. Marine-derived sandy sediments account for a significant part of the infilled volume. The history of infilling, requiring flood-dominant sediment transport, opposes the present-day net ebb-dominance, implying that a change from flood- to ebb-dominance must have occurred during the evolution of the estuary. The ebb-dominance is ascribed to the presence of an extensive high intertidal mangrove area. It is inferred that during the early stages of estuarine evolution, extensive mangrove areas were not present and faster ebb-flows could not be induced. Further expansion of the mangrove area and ongoing evolution of the tidal channels will reinforce the overall ebb-dominance of the estuary.

A similar study in a nearby barrier estuary (Eimeo Creek, Fig. 2) (Lessa, 1994), shows comparable hydrodynamic, morphologic and stratigraphic characteristics to those of Louisa Creek. In addition, morphological analysis of another 30 similar estuaries along this macrotidal coast, made through aerial photos, reveals the recurrence of the three depositional environments identified in this study. It is suggested that the evolutionary history described for Louisa Creek is not a unique case, and may be characteristic of barrier estuaries on macrotidal coasts.

Acknowledgements

We would like to thank Andy Short, Graham Loyd, Skip Davis, Bere Valle, Peter Kerr, Rob Brander, Ian Turner, David Mittchel, Bob Dalrymple and Michael Dubbo for the field assistance during the hydrodynamic and coring campaigns. We would also like to thank Dr. A.D. Short for providing part of the funds for the coring field trip (National Greenhouse Advisory Committee) and Bere Valle for the drawing of the diagrams. We are also grateful to Mary Ferland, Peter Roy, Andy Short and Robert Oaks for their comments on the manuscript. Ocean tide data were provided by the Queensland Department of Transport (DOT) and Beach Protection Authority (BPA). Additional funds were generously provided by the Department of Geography, University of Sydney. Gui Lessa and Gerd Masselink were respectively sponsored by a Brazilian Government scholarship (CNPq) and an Overseas Post-graduate Research Scholarship (OPRS–Australia).

References

Ashley, G.M. and Zeff, M.L., 1988. Tidal channel classification for low-mesotidal salt-marsh. Mar. Geol., 82: 17–32.

Aubrey, D.G. and Speer, P.E., 1985. A study of non-linear tidal propagation in shallow inlet estuarine systems. Part I: Observations. Estuarine Coastal Shelf Sci., 21: 185–205.

Australian National Tide Tables, 1992. Papua, New Guinee and Antarctica. (Aust. Hydrogr. Publ., 10.) Aust. Gov. Publ. Serv., Canberra.

Beach Protection Authority, 1986. Wave Data Recording Programme: Mackay Region. Beach Protection Authority of Queensland (unpubl.).

Black, K.P. and Healy, T.R., 1986. The sediment threshold over tidally induced megaripples. Mar. Geol., 69: 219–234.

Boon, J.D. and Byrne, R.J., 1981. On basin hypsometry and the morphodynamic response of coastal inlets. Mar. Geol., 40: 27–48.

Boyd, R. and Honig, C., 1992. Estuarine sedimentation on the eastern shore of Nova Scotia. J. Sediment. Petrol., 62(4): 569–583.

Bureau of Meteorology, 1965. Climatology of the Pioneer River. Commonwealth of Australia, Director Meteorol., Dep. Supply, 37 pp.

Byrne, R.J., De Alteris, J.T. and Bullock, P.A., 1974. Channel stability in tidal inlets: a case study. Proc. 14th Coast. Eng. Conf. (Copenhagen, Denmark.) ASCE, pp. 1585–1604.

Byrne, R.J. and Boon, J.D., 1976. Speculative hypothesis on the evolution of barrier islands–inlet–lagoon systems. 2. A case study, Wachapreague, Virginia. Geol. Soc. Am., NE SE Sect. Annu. Meet., Abstr., 8: 159.

Dronkers, J., 1986. Tidal asymmetry and estuarine morphology. Neth. J. Sea Res., 20(2/3): 107–131.

Dyer, K.R., 1986. Coastal and Estuarine Sediment Dynamics. Wiley, New York, 342 pp.

Ferland, M.A., 1985. The Stratigraphy and Evolution of the Southern New Jersey Back-barrier Region. Ph.D. Thesis, Rutgers State Univ. New Jersey, 200 pp. (Unpubl.)

Finkelstein, K. and Ferland, M.A., 1987. Back-barrier response to sea-level rise, eastern shore of Virginia. In: D. Nummedal, O.H. Pilkey and J.D. Howard (Editors), Sea-Level Fluctuation and Coastal Evolution. SEPM Spec. Publ., 41: 145–156.

French, J.R. and Stoddart, D.R., 1992. Hydrodynamics of salt-marsh creek systems: implications for marsh morphological development and material exchange. Earth Surface Processes Landforms, 17: 235–252.

Friedrichs, C.T. and Aubrey, D.G., 1988. Non-linear tidal distortions in shallow well-mixed estuaries: a synthesis. Estuarine Coastal Shelf Sci., 27: 521–545.

Friedrichs, C.T., Lynch, D.R. and Aubrey, D.G., 1992. Velocity asymmetries in frictionally-dominated tidal embayments: longitudinal and lateral variability. In: D. Prandle (Editor), Dynamics and Exchanges in Estuaries and the Coastal Zone. Am. Geophys. Union, Washington, Ch. 14, 37 pp.

Fry, V.A. and Aubrey, D.G., 1990. Tidal velocities asymmetries and bedload transport in shallow embayments. Estuarine Coastal Shelf Sci., 30: 453–473.

Gourlay, M.R. and Hacker, J.L.F., 1986. Pioneer River Estuary Sedimentation Studies. Univ. Queensland Printery, Brisbane, 207 pp.

Hegarty, R.A., 1983. Results of a continuous profiling survey in the Mackay area. Geol. Surv. Qld., Record 1983/19 (unpubl.).

Hopley, D., 1983. Evidence of 15,000 years of sea level change in tropical Queensland. In: D. Hopley (Editor), Australian Sea Levels in the Past 15,000 Years. Dep. Geogr., James Cook Univ., Monogr. Ser., pp. 93–104.

Ippen, A.T. and Harleman, D.R.F., 1966. Tidal dynamics in estuaries. In: A.T. Ippen (Editor), Estuary and Coastline Dynamics. McGraw Hill, New York, pp. 493–545.

Kjerfve, B. and Magill, K.E., 1989. Geographic and hydrodynamic characteristics of shallow coastal lagoons. Mar. Geol., 88: 187–199.

Lessa, G.C., 1994. Morphodynamics and evolution of two small macrotidal estuaries—central Queensland, Australia. Ph.D. Dissert., Geogr. Dep., Univ. Sydney, 246 pp.

Lucke, J.B., 1934. A theory of evolution of lagoon deposits on shorelines of emergence. J. Geol., 42: 561–584.

Masselink, G. and Lessa, G.C., 1995. Barrier stratigraphy on the macrotidal Central Queensland coastline. J. Coastal Res., 11(2): 454–477.

Mota-Oliveira, I.B., 1970. Natural flushing ability in tidal inlets. Proc. 12th Coastal Eng. Conf. (Washington, D.C.) ASCE, pp. 1827–1845.

Myrick, R.M. and Leopold, L.B., 1963. Hydraulic geometry of a small tidal estuary. U.S. Geol. Surv. Prof. Pap., 422B: 1–18.

Newman, W.S. and Munsart, C.A., 1968. Holocene geology of the Wachapreague lagoon, eastern shore peninsula, Virginia. Mar. Geol., 6: 81–105.

Nichols, M.M., 1989. Sediment accumulation rates and relative sea-level rise in lagoons. Mar. Geol., 88: 201–219.

Oertel, G.F., Kraft, J.C., Kearney, M.S. and Woo, H.J., 1992. A rational theory for barrier–lagoon development. In: Quaternary Coasts of the United States: Marine and Lacustrine Systems. SEPM Spec. Publ., 48: 77–87.

Pethick, J.D., 1991. Tidal and estuarine management in the Humber Estuary, England. Proc. Coastal Zone '91, pp. 1456–1468.

Roy, P.S., 1984. New South Wales estuaries: their origin and evolution. In: B.G. Thom (Editor), Coastal Geomorphology in Australia. Academic Press, Sydney, pp. 99–121.

Speer, P.E. and Aubrey, D.G., 1985. A study of non-linear tidal propagation in shallow inlet/estuarine systems. Part II: theory. Estuarine Coastal Shelf Sci., 21: 207–224.

Thom, B.G. and Roy, P.S., 1983. Sea level change in New South Wales over the past 15,000 years. In: D. Hopley (editor), Australian Sea Levels in the Past 15,000 years. Dep. Geogr., James Cook Univ., Monogr. Ser., pp. 64–84.

Wright, L.D. and Thom, B.G., 1977. Coastal depositional landforms: a morphodynamical approach. Progr. Phys. Geogr., 1: 412–429.

Wrigth, L.D., Coleman, J.M. and Thom, B.G., 1973. Process of channel development in a high-tide-range environment: Cambridge Gulf–Ord River delta, Western Australia. J. Geol., 81: 15–41.